AD-A237 606

(2)

CUMENTATION PAGE

Form Approved OMB No. 0704-0188

1b RESTRICTIVE MARKINGS: NA	
2a SECURITY CLASSIFICATION AUTHORITY: NA	3 DISTRIBUTION/AVAILABILITY OF REPORT: Distribution Unlimited
2b DECLASSIFICATION/DOWNGRADING SCHEDULE: NA	
4 PERFORMING ORGANIZATION REPORT NUMBER(S): TSI Mason Research Institute #4193- 4	5 MONITORING ORGANIZATION REPORT NUMBER(S): NA
6a NAME OF PERFORMING ORGANIZATION: TSI Mason Research Institute; 6b OFFICE SYMBOL (If applicable): Biochemistry	7a NAME OF MONITORING ORGANIZATION: Office Of Naval Research
6c ADDRESS (City, State, and ZIP Code): 57 Union Street, Worcester, MA. 01608	7b ADDRESS (City, State, and ZIP Code): 800 N. Quincy Street, Arlington, VA 22217-5000
8a NAME OF FUNDING/SPONSORING ORGANIZATION: Office of Naval Research; 8b OFFICE SYMBOL (If applicable): ONR	9 PROCUREMENT INSTRUMENT IDENTIFICATION NUMBER: N00014-88-C-0193
8c ADDRESS (City, State, and ZIP Code): 800 N. Quincy Street, Arlington, VA 22217-5000	10 SOURCE OF FUNDING NUMBERS: PROGRAM ELEMENT NO 61153N; PROJECT NO 1113ES; TASK NO 413K003; WORK UNIT ACCESSION NO

11 TITLE (Include Security Classification)

Evaluation of Surface-Bound Membranes with Electrochemical Impedance Spectroscopy

12 PERSONAL AUTHOR(S)
Jianguo Li, Nancy W. Downer and H. Gilbert Smith

13a TYPE OF REPORT	13b TIME COVERED	14 DATE OF REPORT (Year, Month, Day)	15 PAGE COUNT
Technical	FROM _____ TO _____	91.6.6	39

16 SUPPLEMENTARY NOTATION

Submitted for an ACS Advances in Chemistry volume on Membrane Electrochemistry

17 COSATI CODES			18 SUBJECT TERMS (Continue on reverse if necessary and identify by block number)
FIELD	GROUP	SUB-GROUP	AC Impedance, Biomembrane, Lipid, Receptor Protein, Electrode, Biosensor

19 ABSTRACT (Continue on reverse if necessary and identify by block number)

Membrane structures containing the visual receptor protein, rhodopsin, were formed by detergent dialysis on platinum, silicon oxide, titanium oxide and indium/tin oxide electrodes. Electrochemical impedance spectroscopy was used to evaluate the biomembrane structures and their electrical properties. A model equivalent circuit is proposed to describe the membrane electrode interface. The data suggest that the surface structure is a relatively complete single membrane bilayer with a coverage of 0.97, and with longterm stability.

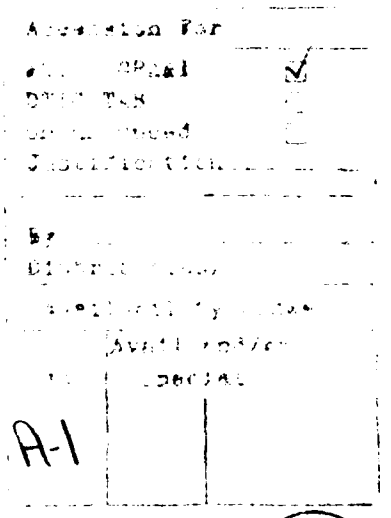
20 DISTRIBUTION/AVAILABILITY OF ABSTRACT: ☒ UNCLASSIFIED/UNLIMITED ☐ SAME AS RPT ☐ DTIC USERS	21 ABSTRACT SECURITY CLASSIFICATION: U
22a NAME OF RESPONSIBLE INDIVIDUAL: Dr. R.J. Nowak/Dr. I. Vodyanoy	22b TELEPHONE (Include Area Code): (703) 696-4409/4056; 22c OFFICE SYMBOL: ONR

OFFICE OF NAVAL RESEARCH

Contract N00014-88-C-0193

R&T Code 413k003

Technical Report No. 4



Evaluation of Surface-Bound Membranes with Electrochemical Impedance Spectroscopy

by

Jianguo Li, Nancy W. Downer and H. Gilbert Smith

Submitted
for an
ACS Advances in Chemistry
volume on
Membrane Electrochemistry

TSI Mason Research Institute
Biochemistry Department
57 Union St.
Worcester, MA 01460

June 6, 1991

Reproduction in whole, or in part, is permitted for any purpose of the United States Government.

This document has been approved for public release and sale; its distribution is unlimited.

91 6 18 046

91-02457

Evaluation of Surface-Bound Membranes With Electrochemical Impedance Spectroscopy

Jianguo Li, Nancy W.Downer and H. Gilbert Smith

TSI Mason Research Institute
57 Union St., Worcester, MA 01608
(508) 791-0931

ABSTRACT

Membrane structures containing the visual receptor protein, rhodopsin, were formed by detergent dialysis on platinum, silicon oxide, titanium oxide and indium/tin oxide electrodes. Electrochemical impedance spectroscopy was used to evaluate the biomembrane structures and their electrical properties. A model equivalent circuit is proposed to describe the membrane electrode interface. The data suggest that the surface structure is a relatively complete single membrane bilayer with a coverage of 0.97, and with longterm stability.

INTRODUCTION

Communication in living organisms is governed by the cell bilayer membrane, which selectively recognizes specific chemical messengers in the presence of others and responds accordingly. Receptor proteins located in cellular membranes have evolved for highly specific recognition functions and are the natural sites of action for a wide variety of biologically active chemical components including hormones, neurotransmitters, odorants and many drugs.

Biosensors based upon membrane receptors require the protein to be coupled both functionally and structurally with electrical substrates. The interface between the biological recognition element and the solid substrate must allow electrical signal transduction and provide an environment conducive to biological function. Both requirements are demanding. A significant barrier to producing this type of sensor has been the tremendous difficulty of preparing functional and stable lipid/protein bilayer membranes linked to surfaces. Such membranes should be functionally equivalent to free-standing membranes, and must (1) provide a "blocking" interface to prevent unintended permeabilities, (2) be chemically and mechanically stable on solid substrates, and (3) incorporate specific protein receptors.

Receptor proteins normally function as part of the lipid bilayer membrane that separates intracellular and extracellular aqueous compartments. Proteins in natural membranes are thus exposed to regions of two different compositions: the high dielectric, aqueous media at the surface of the membrane, and the low dielectric, hydrophobic, hydrocarbon region at the core of the lipid bilayer.

Several procedures have been developed for forming artificial membranes that retain properties of natural biological membranes [1,2]. These procedures rely upon the self-assembly properties of the membrane components (lipids and proteins) to form functioning membrane structures. Lipid bilayer structures have been formed by sonicating suspensions of lipids to form

vesicles [3], spreading dissolved lipids across an orifice to form planar bilayer [4], and by using Langmuir-Blodgett techniques to serially add monolayers to a surface [5]. Although Langmiur-Blodgett techniques offer good control in depositing a membrane lipid phase onto solid surfaces, the techniques for inserting membrane proteins are less well developed.

Various procedures have been used to incorporate membrane proteins into these lipid bilayer structures. These include the fusion of protein-containing vesicles with planar lipid bilayers [6], and the use of detergent dilution techniques to insert proteins into unilamellar vesicles [7]. For the simultaneous assembly of membranes, detergent dialysis has been used to directly form protein-containing bilayer membrane vesicles from solubilized protein-lipid mixture [8,9].

We have reported the formation of surface-bound lipid membranes containing receptors on planer electrode surfaces by a modified detergent dialysis technique [10]. The first step in our approach is to covalently form a hydrophobic monolayer with long hydrocarbon chains onto electrode surfaces by alkylsilanization. Such a hydrophobic surface can be thought of as one leaflet of a membrane bilayer. The second leaflet of the bilayer is then deposited by detergent dialysis which allows protein to incorporate simultaneously with the deposition of lipid. Our hypothesis is that the hydrocarbon chains attached to the surface serve as initiation sites for a lipid bilayer membrane to form as the detergent is removed. The model is of a

membrane that is anchored to the surface by hydrophobic interactions with the surface-bound hydrocarbon layer.

Membranes containing the visual pigment, rhodopsin, a G-proteins linked receptor, have been chosen as a model system for this work. Rhodopsin was one of the first integral membrane proteins whose amino acid sequence was determined [11]. More than 40 receptors have been reported having structural and functional homologies with rhodopsin [12]. This paper describes the use of electrochemical impedance spectroscopy to evaluate lipid bilayer membranes containing rhodopsin formed on electrode surfaces.

EXPERIMENTAL

Chemicals and biochemicals Acetonitrile (ACN, 99%), tetrabutylammoniumtetrafluoroborate (TBAF, 99%), tetracyanoethylene (TCNE, 98%) and anhydrous n-hexadecane (99%) were from Aldrich and used as received. Chloroform (American Burdick & Jackson) and carbon tetrachloride (Mallinckrodt) were dried over aluminum oxide (Water Associates, Framingham, MA) for at least 48 hours before use. Octadecyltrichlorosilane (OTS) and dimethyloctadecylchlorosilane (DMOCS) were from Petrach System, Inc., Bristol, PA. KCl, H_2SO_4 and HF (52%) were of AR grade from Mallinckrodt. N-2-hydroxyethylpiperazine-n'-ethanesulfonic acid (HEPES, pKa 7.55) was from Sigma. Octyl-β -D-glucopyranoside (OG) used as detergent was from Calbiochem, La Jolla, CA. Disk membranes containing rhodopsin (Rh) were isolated from rod outer

segments from bovine retinas (J.A. Lawson, Co., Lincoln, NE) by flotation on 5% ficoll [13]. Platinum sheet (99.99%) and titanium rod (99.99%) were purchased from Johnson Matthey. p-Si (24-36 ohm-cm) and n-Si (100 ohm-cm) wafers with a silica layer thickness of 950 Å on the polished side and a gold film evaporated on the other side were provided by EG&G Reticon, Sunnyvale, CA. Indium/tin oxide (100-500 Å thick) coated glass substrate (ITO) was from Donnelly Co., Holland, Michigan.

Electrode preparation Pt electrodes were polished with alumina polishing powder (1 μm, 0.3 μm, 0.05 μm) to a mirror finish and cleaned electrochemically by cycling the potential between hydrogen and oxygen evolution potentials in 1 M H_2SO_4 until the characteristic clean Pt wave pattern of hydrogen adsorption was observed. The electrode was next poised at 1.1 V vs SCE until the current decayed to a small value indicating complete oxidation of the electrode surface.

The titanium electrodes were polished with diamond paste (1 μm, 0.3 μm) in mineral oil and washed in acetone followed by deionized water. The TiO_2 film was formed on titanium in 1 M H_2SO_4 while the potential was swept slowly in a positive direction at a sweep rate of 1 mV/s. The thickness of the anodic film was proportional to the growth voltage applied. Anodizing ratios for titanium at 1 mV/s sweep rate are reported to be 6 nm/V up to 2 V and 3.6 nm/V above 2 V [14]. In this work, the growth potential was 3 V vs SCE and the thickness was estimated to be 15 nm.

The silicon oxide electrodes were 5mm x 5mm chips cut from a Si/SiO_2 wafer. The ohmic contact was made by connection of a wire to the gold film on the rear side of the chip with silver conducting epoxy. The chip was then mounted on a glass tube and sealed along its edge with epoxy. An etching process to reduce the SiO_2 thickness was carried out in 5% HF at room temperature.

The ITO electrode was made of a 5mm x 5mm slice cut from ITO sheet. A copper wire was attached to the ITO film with silver conducting epoxy. The ITO slice was mounted on a glass tube with epoxy. All electrodes were washed thoroughly with deionized water and vacuum oven-dried for 12 hours at 100°C before alkylsilanization.

Alkylsilanization Alkylsilanization of electrode surfaces was carried out by a modification of the procedure of Sagiv [15]. The anhydrous solvent was prepared with 80:12:8 hexadecane: chloroform: carbon tetrachloride under dried nitrogen in a glove bag (relative humidity < 4%). The dried electrodes were silanized by reaction in stirred 3% (V/V) OTS solution for 3 hours or 6% (V/V) DMOCS solution for 6 hours. The silanized electrode surface was rinsed with dry solvent and then with chloroform and cured in a vacuum oven at 100°C for 12 hours.

Detergent dialysis The technique of detergent dialysis, which is often used to form functional membrane vesicles [8,9], was adopted to assemble membrane-mimetic structure onto electrode surfaces. The dialysis unit used in this work had two compartments separated by dialysis membrane filter (Spectra/Pro 6

membrane, molecular weight cutoff 3500, Los Angeles, CA). The electrode was mounted in one compartment that contained detergent solubilized disk membranes. Dialysis was against a flowing stream of detergent-free buffer driven by a peristaltic pump (type 2232 Microperpex s, LKB, Sweden). Rod outer segment disk membranes were solubilized with 30 mM OG to a final rhodopsin concentration of 1 mg/ml. Care was taken to avoid bubbles in the dialysis compartments. The detergent dialysis was carried out at 4°C in the dark or under red light filtered through a Kodak #2 safe light filter (Eastman Kodak Co.). The detergent dialysis was at a flow rate of 100 μl/min for 20 - 30 hours.

Electrochemical measurements Cyclic voltammetry and AC impedance spectroscopy were performed using an EG&G Princeton Applied Research Model 378 AC Impedance System that included a model 273 potentiostat/galvanostat, a model 5208 two-phase lock-in analyzer and a IBM PS/2 computer. For AC impedance measurements, a sine wave of 5 mV (RMS) was superimposed on an applied DC bias from the potentiostat. Reference electrodes used were saturated calomel electrodes (SCE) (Fisher) for measurements in aqueous solution and silver electrodes for measurements in non-aqueous solution. All potentials are reported with respect to SCE.

RESULTS AND DISCUSSION

Surface modification with organosilanes

It is known from chromatographic [16] and other studies that the order of reactivity of halosilanes with silica is X_3SiR > X_2SiR_2 > $XSiR_3$. This relationship was also observed with SnO_2 surfaces [17] based upon an ESCA analysis. Organosilanes with more than one reactive group have the potential of binding to more than one surface site but also can cross react to form polymers. Boucher et al [18], for instance, demonstrated during the immobilization of diphenylphosphine groups on silica that the trichlorosilane reagent claimed slightly less than two sites per silane. The fate of the remaining silane reactive group is important to the surface structure formed. Aue, Hastings et al [19,20] claim that linear siloxane polymers form that are bound to the silica surface at only a few sites. Polymer formation can occur if, after a dichloro or trichlorosilane forms one -Si-O-Si- surface link, a second Si-Cl bond becomes hydrolyzed by water forming -Si-O-Si(OH)-. If this occurs in the presence of unreacted solution chlorosilane, a polymer chain can be initiated at the Si(OH) site. Such polymer formation can occur on most metal oxide surfaces.

Pt electrode anodization in sulfuric acid at 1.1 V and 1.9 V vs. SCE yields an approximate monolayer of PtO and a surface layer of predominantly PtO_2, respectively [21,22]. It was reported that Pt electrodes anodized at 1.1 V can be silanized

under anhydrous condition [23] producing surface Pt-O-Si- bonds. We have used the X_3SiR and $XSIR_3$ silanes, OTS and DMOCS, to modify the surface of our electrodes. It was found that X_3SiR silane produced a more stable and reproducible silane layer on electrode surfaces. We have therefore employed octadecyltrichlorosilane (OTS) to obtain high surface coverages for supporting the reconstituted membrane structure. OTS has a C_{18} carbon chain with a length of 26.5 Å, which is approximately equivalent to a single lipid layer of a membrane bilayer structure. In order to form a single layer of OTS on the electrode surfaces we have attempted to minimize polymer formation by utilizing dry solvents, and by carefully and thoroughly washing excess silane from the electrode with fresh solvent before exposing the electrode to moisture.

Electrochemical analysis of PtO/OTS electrodes

OTS forms a neutral and low dielectric silane layer, and is electrochemically inert. The OTS layer formed on Pt electrodes acts as an insulating layer, blocking the active Pt surface. Electrochemical examination of the PtO/OTS electrode provides information on the structure of the OTS layer on which the lipid/protein membrane is formed. We have examined the PtO/OTS electrode surface in a non-aqueous electrolyte (to avoid reduction of PtO) using tetracyanoethylene (TCNE) as the model redox species.

Cyclic voltammograms of TCNE at Pt oxide and PtO/OTS

electrodes measured at the sweep rate of 40 mV/s in 0.1 M TBAF in acetonitrile are shown in figure 1. The well defined pair of chemically reversible waves measured at the Pt oxide electrode, which represent reduction of TCNE to its anion and reoxidation of the anion to TCNE, exhibit the 60 mV peak potential separation and wave symmetry expected for a reversible electrochemical reaction. For the PtO/OTS electrode, the reduction and oxidation peak currents of TCNE decrease dramatically. The peak potential separation increases to 180 mV indicating irreversibility of TCNE at the PtO/OTS electrode. The Pt electrode is still accessible to reduction and oxidation of TCNE after OTS coating, but the effective (microscopic) electrode area appears to be lowered by the covalent bonding of OTS to the Pt surface. The smaller microscopic area gives rise to higher current densities, an increased charge transfer rate limitation and irreversibility. This suggests that a porous OTS layer is formed on the Pt oxide electrodes.

The porous structure of the OTS layer on PtO was confirmed by the electrochemical impedance spectra of TCNE. Figure 2 shows the complex plane plots of TCNE reduction at Pt oxide and PtO/OTS electrodes at -0.4 V, near the TCNE reversible potential, where Z' and Z'' are the real and imaginary components of the measured impedance respectively. A complex plane plot with a semicircle and a 45 degree tail was measured at the PtO electrode. This is the normal plot expected for a charge transfer process at a smooth electrode surface [24-26]. The PtO/OTS electrode, however,

gave a sunken semicircle in the measured complex plane plot. This may be indicative of a porous electrode surface. For a rough electrode surface the uncontrolled nature of surface roughness makes it difficult to describe mathematically. Fractal analysis has been used to describe diffusion at a rough electrode surface and sunken semicircular curves have been simulated [27-29]. The sunken semicircle measured with the PtO/OTS electrode may suggest fractal surface features with pores of different sizes and shapes permeating through the OTS layer to the electrode surface.

The effective area of the OTS coated Pt oxide electrode can be derived if the charge transfer resistance (R_{ct}) is known. R_{ct} can be obtained from impedance data measured at a potential near the reversal potential [30,31]. $R_{ct} = RT/(nFAI)$, where I is the exchange current density and A the effective surface area. Since the impedance spectra of the Pt oxide and PtO/OTS electrodes were measured under the same conditions, the value of R_{ct} may be assumed to be affected only by the effective surface area. In figure 3, the impedance data are rearranged and plotted as Z' vs $1/\omega^{1/2}$. R_{ct} is estimated from the intercept on the Z' axis by extrapolation. The R_{ct} values are 95 and 980 ohms for PtO and PtO/OTS, respectively. An OTS coverage factor, θ, can then be estimated from $(1-\theta) = R_{ct(PtO)}/R_{ct(PtO/OTS)}$. In this case θ is equal to 0.9.

The electrochemical stability of PtO/OTS in aqueous saline solution was tested by measuring cyclic voltammograms of PtO and PtO/OTS electrodes in 0.1 M KCl, pH 6.8 (figure 4). The

electrode capacitances corresponding to the cyclic voltammograms are shown in figure 5. These were measured at 1000 Hz. The OTS layer can be described as a planar capacitor in series with the PtO and double layer capacitances. Formation of the OTS layer decreased the capacitance; however, the Pt oxide beneath the OTS layer was still reduced when the potential was swept below 0.3 V. This again is evidence that the OTS layer on PtO is somewhat porous. The onset potential of PtO reduction in aqueous solution is pH dependent.

The OTS layer was found to be chemically unstable at pH > 9. At this pH, the capacitance immediately increased to the value of the bare PtO electrode suggesting that the OTS layer dissolves in basic solutions. The hydrolysis of silane on SiO_2 has been previously observed in 0.1 M NaOH [17]. The silane Pt oxide is reported to be resistant to most solvents including dilute aqueous acid (for a few minutes) [23]. Our measurements confirm the stability on PtO at neutral pH.

For characterizing the membrane coated Pt electrodes we have chosen a potential window from 0.3 to 0.6 V where PtO is electrochemically stable and passive according to the cyclic voltammograms in Figure 4. The pH was 6.8.

Electrochemical properties after membrane deposition

A rhodopsin-containing membrane was deposited on PtO/OTS electrodes by dialysis as described in the Experimental section. After dialysis, the electrodes were gently rinsed with saline

buffer to wash off excess vesicles on the surface before electrochemical measurements. The changes in the cyclic voltammogram and the capacitance are illustrated in figure 4 and figure 5. Deposition of the membrane on the electrode surface brought about further "blocking" of the effective area of PtO, resulting in a further suppression of the PtO reduction (see figure 4). The capacitance decreased further as the result of an additional capacitance due to the rhodopsin containing membrane in series with the existing capacitance of oxide and OTS layers (see figure 5).

Impedance spectra were recorded in 0.1 M KCl, pH 6.8, at 0.4 V vs SCE. Figure 6 shows the Bode plots of log $|Z|$ vs log f and phase angle (θ) vs log f, where $|Z|$ is the impedance magnitude, f is the frequency, and phase angle is the arc tangent of the ratio of the imaginary and real parts of the measured impedance. The magnitude of the impedance increased upon membrane formation and the phase angle was also sensitive to membrane deposition. A broad phase angle maximum plateau appeared in the frequency range > 500 Hz, but disappeared after washing the electrode with 30 mM OG to dissolve the deposited membrane (see the half-opened dot curve in figure 6). These results are consistent with a protein/lipid membrane being formed on the OTS-treated Pt oxide electrode by detergent dialysis.

Model of surface-bound membrane on Pt electrode

From the experimental results discussed above one can

develop a physical model of the surface-bound membrane consisting of two layers as schematically depicted in figure 7. The porous, hydrophobic OTS layer provides a structure to anchor the reconstituted membrane layer. Protein molecules with bound lipid may insert into the pores in the OTS layer. The model assembly is essentially a bilayer membrane immobilized on the electrode surface.

More detailed information on the physical structure and electrical properties can be obtained by analysis of the impedance spectra presented in figure 6. An equivalent circuit can be derived for the surface-bound membrane similar to the approach taken for porous anodic films and porous electrodes [31]. An equivalent circuit network is proposed in figure 8a, corresponding to the model in figure 7. This has three RC subnetworks representing the oxide layer, the surface-bound membrane layer and the double layer. C_{ox} and R_{ox} are the capacitance and resistance of oxide. C_{dl} and R_{dl} are the double layer capacitance and Warburg resistance at the membrane/water interface. For the subnetwork of the surface-bound membrane layer, one branch represents a tightly packed alkylsilane and lipid bilayer in series, and the other branch represents the pores and defects through the bilayer. C_{alk}, C_{lip} and R_{alk}, R_{lip} are the capacitances and resistances of alkylsilane and lipid layers. R_{el} is the resistance of electrolyte in series with the RC circuit of the double layer at the oxide/water interface in the pores. R_u is the series resistance of the electrolyte. θ is

defined as the coverage factor for the tightly packed bilayer on the surface and (1-θ) is the fractional area covered by pores and defects.

The simulation spectra of the Pt oxide electrodes with and without the surface-bound membrane are shown in figure 9 for comparison with the experimental data. The parameters used in the simulation are listed in Table 1. The first column lists the values used for curve fitting the experimental spectra, and the second column gives the corresponding values normalized for unit area.

This simulation reproduces the essential features of the experimental data. A calculated capacitance for the tightly packed part of the surface-bound membrane (C_{bl}) can be obtained by treating C_{alk} and C_{lip} in series. The resistance can be similarly calculated from R_{alk} and R_{lip}. The calculated values of 0.52 $\mu f/cm^2$ and 1325 ohms-cm^2 are in good agreement with literature values for natural membranes. The best curve fit for the coverage factor, θ, was 0.97, indicating formation of a relatively complete membrane by the detergent dialysis approach.

Capacitance values of the Pt oxide, C_{ox}, and double layer, C_{dl}, from the best curve fit are lower for the membrane-coated electrode than for the bare PtO electrode. Also the resistances are higher for the membrane-coated electrode than for the bare PtO electrode. The structure of the oxide and the double layer is probably altered by membrane deposition. For example, the hydrophobic alkylsilane layer may dehydrate the oxide layer, and

may expand the double layer making it more diffuse.

The impedance response of each layer on the electrode surface can probably be identified on the spectrum in terms of frequency. Although the broad phase angle maximum plateau induced by the formation of the surface-bound membrane on the PtO electrode is attributed to several RC constants, the total impedance is dominated by the admittance of the surface-bound membrane for frequencies > 500 Hz. Typical double layer capacitances are usually in the range of 10 - 40 $\mu f/cm^2$, which is at least an order of magnitude greater than the membrane capacitance. Thus at higher frequencies, the double layer capacitance behaves as a short circuit and can be neglected. In addition, R_{ox}, R_{alk}, R_{lip} and R_{dl} are usually in the range of 1 - 100 kΩ, and are higher than the impedances of the capacitance components in the equivalent circuit. They can be treated as open circuits at higher frequencies. Rel is small and can be treated as a short circuit. R_u can be either compensated experimentally or subtracted in the data analysis. The equivalent circuit in figure 8a can therefore be simplified as shown in figure 8b.

In this simplified form, the membrane capacitance, C_m, is in series with C_{ox}. Thus, $C_m = C_{ox} \cdot C_t/(C_t - C_{ox})$, where C_t is the total capacitance of the surface-bound membrane electrode and C_{ox} is the measured capacitance of the electrode before membrane formation. The membrane capacitance, C_m, can thus be estimated at a single frequency. Further, the capacitance of the tightly packed bilayer, C_{bl}, can be calculated from C_m if the coverage

factor and the double layer capacitance are known: $C_{bl} = (C_m - (1-\theta) \cdot C_{dl})/\theta$. Using the imaginary component of the measured impedance data for PtO/OTS and PtO/OTS/Rh electrodes at a frequency of 1000 Hz (after subtracting R_u), the calculated C_m is 867 nf/cm^2 and C_{bl} is thus 584 nf/cm^2 using C_{dl}=10 μf/cm^2 and θ = 0.97, which are close to the theoretical values derived from the best curve fit simulation. It is concluded that the simplified equivalent circuit may be adequate for the surface-bound membrane electrode. The thickness of the tightly packed membrane bilayer,d, can be calculated from $d=\varepsilon_0\varepsilon/C_{bl}$, where ε is the dielectric constant of the bilayer. The calculated thickness of the membrane bilayer on the PtO electrode is 46.8 Å using a dielectric constant of three.

Surface-bound membranes formed on Pt oxide electrodes were chemically and mechanically stable. The PtO/OTS/Rh electrodes were monitored by measuring the capacitance while the electrodes were kept in buffer at 4°C for 11 days. Any dissolution of the surface-bound membrane would result in an increase in capacitance. Little change in capacitance was observed indicating that the membranes are stable.

Surface-bound membrane on SiO_2, TiO_2 and ITO electrodes

The detergent dialysis procedure was also used to deposit membranes on SiO_2, TiO_2 and ITO electrodes. The planar Si/SiO_2 electrode is a solid-state capacitor with the n- or p-type silicon substrate forming one "plate" of the capacitor and the

electrolyte at the surface forming the other plate. The insulating SiO_2 layer and surface-bound membrane form the dielectric. Although a simple device, the planar Si/SiO_2 electrode has the same fundamental physical structure as other solid-state devices, such as field effect transistors (FETs), but allows a simpler approach to analyzing the device characteristics. For example, the FET sensor relies on changes in its gate voltage caused by a change in the surface charge density upon exposure to an analyte. The gate of the FET is operated under inversion condition and can be represented by an equivalent circuit of space charge capacitance, silicon oxide layer capacitance and membrane capacitance in series. All three capacitances must be considered in analyzing the device response. In contrast, the Si/SiO_2 electrode can be operated under accumulation condition and only the silicon oxide and membrane capacitances need to be considered. SiO_2 is extremely stable in most biological solutions and suitable for alkylsilanization. The capacitance of a 950 Å thick SiO_2 layer is typically 35 nf/cm^2, which is one order lower than that of the surface-bound membrane. The total impedance of the electrode is therefore dominated by the SiO_2 capacitance.

TiO_2 formed by electrochemical anodization on a polished titanium surface is usually an n-type semiconductor. In the potential window where it is passive, TiO_2 is in a depletion condition. The capacitance of TiO_2 is the space charge capacitance described by the Mott-Schottkey equation.

ITO electrodes behave electrochemically similar to Pt electrodes and the double layer capacitance can be neglected at higher frequencies allowing one to easily calculate the membrane capacitance.

The simplified equivalent circuit in figure 8b was used to evaluate surface-bound membranes on SiO_2, TiO_2 and ITO electrodes. Figures 10 and 11 present the capacitance curves for n-Si/SiO_2 and TiO_2 electrode with and without OTS and rhodopsin containing lipid membranes in KCl buffer. As with the PtO electrodes, the capacitance decreases upon formation of an OTS layer and the membrane on the oxide surface. Table 2 lists the measured capacitances (C-total) for the unmodified electrodes, and for the electrodes after alkylsilanization and membrane deposition. From these measured values we have used the simplified equivalent circuit of figure 8b to calculate the capacitance of the OTS layer and the combination of the OTS layer and deposited membrane. Adjusting the latter for the surface coverage, θ, provides the capacitance of the tightly packed bilayer, C_{bl}, from which the thickness of the surface-bound membrane is calculated. These results are all consistent with a single membrane bilayer being formed on the electrode surfaces.

Since the surface-bound membrane capacitance is in series with the oxide layer capacitance, the change in the total capacitance induced by the surface-bound membrane is a function of both the dielectric properties and the thickness of the oxide layer. The dielectric constants for TiO_2 and ITO are 10 - 15

times higher than for SiO_2, thus a larger change in capacitance is observed when the membrane is formed on TiO_2 and ITO electrodes than with the SiO_2 electrode (see Table 2). The SiO_2 thickness of the p-Si/SiO_2 electrode was 550 Å (reduced from 950 Å by etching in HF). The n-Si/SiO_2 electrode had a 950 Å oxide layer. As shown in Table 2, the thinner the SiO_2 on the p-type silicon electrodes, the larger the change in capacitance upon membrane formation. The calculated capacitance of the surface-bound membrane itself on the p-Si/SiO_2 electrode is lower than for the other electrodes. This may indicate formation of a tighter membrane bilayer. The etching may provide a cleaner hydrated surface for better alkylsilanization and membrane deposition.

CONCLUSIONS

Electrochemical impedance spectroscopy provides a sensitive means for characterizing the structure and electrical properties of the surface-bound membranes. The results from impedance analysis are consistent with a single biomembrane- mimetic structure being assembled on metal and semiconductor electrode surfaces. The structures formed by detergent dialysis may consist of a hydrophobic alkyl layer as one leaflet of a bilayer and the lipid deposited by dialysis as the other. Proteins surrounded by a bound lipid layer may simultaneously incorporate into pores in the alkylsilane layer by hydrophobic interactions during deposition of the lipid layer.

ACKNOWLEDGEMENTS

This research supported in part by the Office of Naval Research.

REFERENCES

1. Darszon, A., J. Bioenerg. Biomemb., 1983, **15**, 321.
2. Montal, M.,Biochim. Biophys. Acta, 1979, **559**, 231.
3. Huang, C., Biochemistry, 1969, **8**, 344.
4. Mueller, P., Rudin, O.O., Tien, H.T. and Westcott, W.C., Nature, 1962, **194**, 979.
5. Procarione, W. L. and Kauffman, J.W., Chem. Phys. Lipids, 1974, **12**, 251.
6. Miller, C., Physiological Review, 1983, **63**, 1209.
7. Jackson, M.L. and Litman, B.J., Biochem., 1982, **21**, 5601.
8. Madden, T.O., 1986, Chem. Phys. Lipids, **40**, 207.
9. Kagawa, Y. and Racker, E., J. Biol. Chem., 1971, **246**, 5477.
10. Smith, H.G., Li, J., Downer, N.W., and Deluca, L.W., Proc. IEEE/EMBS, 1989, Vol.11, 1329
11. For example: Ovchinnikov, Y.A., Abdulaev, N.G., Feigina, M.Y., Artamonov, I.D., Zolotarev, A.S., Kostina, M.B., Bogachuk, A.S., Miroshinikov, A.I., Martinov, V. I. and Kudelin, A.B., Bioorg. Khim., 1982, **8**, 1011; Hargrave, P.A., McDowell, J.H., Curtis, D.R., Wang, J.K., Jusczak,E., Fong, S.-L., Rao, J.K.M. and Argos, P., Biophys. Struct. Mech., 1983, **9**, 235; Nathans, J. and Hogness, D.S., Cell, 1983, **34**, 807.

12. Birnbaumer,L., Abramowitz, J., and Brown, A.M., Biochim. et Biophys. Acta, 1990, **1031**,1063.

13. Smith, H.G. and Litman, B.J. Enzymol. 1982, **81**, 57.

14. McAleer, J.F. and Peter, L.M., Faraday Disc. Royal Soc. Chem, 1980, **70**, 67.

15. Sagiv, J., J. Am. Chem. Soc., 1980, **102**, 92.

16. Grushka, E., Ed, Bonded Stationary Phases in Chromatography, Ann Arbor Science Pub., Ann Arbor, Mich.,1974.

17 Moses, P.R., Wier, L. and Murray, R., Anal. Chem., 1975, **47**, 1882.

18. Oswald, A.A., Murrel, L.L. and Boucher, L.J., Abstracts Div. Petroleum Chem., 168th ACS meeting, Los Angeles, CA., 1974.

19. Aue, W.A. Hastings, C.R., Augl, J.M., Norr, M.K. and Larsen, J.V., J. Chromatogr., 1971, **56**, 295.

20. Aue, W.A., Hastings, C.R., J. Chromatogr., 1969, **42**, 319.

21. Allen, G.C., Tucker, P.M., Capon, A. and Parsons, R., J. Electroanal. Chem., 1974, **50**, 335.

22. Kim, K.S., Winograd, N., Conway, R.E. and Davis, R.E., J. Am. Chem. Soc., 1971, **93**, 6296.

23. Lenhard, J.R. and Murry, R.W., J. Electroanal. Chem., 1977, **78**, 195.

24. de Levie, R. and Pospisil, L., J. Electroanal. Chem., 1969, **22**, 277.

25. de Levie, R., J. Electroanal. Chem., 1990, **261**, 1.

26. Maritan, A. and Toigo, F., Electrochim. Acta, 1990, **35**, 141.

27. de Gennes, P.-G., Compt. Rend. 1982, **295 (2)**, 1061.

28. Nyikos, L. and Pajkossy, T., Electrochim. Acta, 1985, **30**, 1533.

29. de Levie and Vogt, A., J. Electroanal. Chem., 1990, **278**, 25.

30. Bond, A.M., Modern Polarographic Methods in Analytical Chemistry, Marcel Dekker, New York, 1980.

31. Macdonald, D.D., Transient Techniques in Electrochemistry, Plenum, New York, 1977.

32. For example: Madon, M.J. and Mckubre, M.C.H., J. Electrochem. Soc., 1983, **130**, 1056; Lenhart, S.L., Macdonald, D.D. and Pownd, B.G., J. Electrochem. Soc., 1988, **135**, 1063; Mansfeld, F. and Kendig, M.W., J. Electrochem. Soc., 1988, **135**, 828; Hoar, J.P.and Wood, G.C., Electrochim. Acta 1962, **7**, 333; Hitzig, J., Juttner, K., Lorenz, W.J. and Paatsch, W., Corros. Sci., 1984, **24**, 945.

Figure Legends

Fig. 1 Cyclic voltammetry of tetracyanoethylene (TCNE) on the PtO and PtO/OTS electrodes at 40 mV/s. 5 mM TCNE in acetonitrile containing 0.1 M TBAF.

Fig. 2 Complex plane plots of TCNE reduction on the PtO and PtO/OTS electrodes at -0.4 V in 5mM TCNE in acetonitrile containing 0.1 M TBAF.

Fig. 3 Z' vs $\omega^{-1/2}$ Plots for the impedance data from figure 2. The uncompensated electrolyte resistance of 150 ohms is subtracted.

Fig. 4 Cyclic voltammetry of the PtO, PtO/OTS and PtO/OTS/Rh electrodes in 0.1 M KCl containing 20 mM HEPES, pH 6.8. The sweep rate is 20 mV/s.

Fig. 5 Capacitances of the PtO, PtO/OTS and PtO/OTS/Rh electrodes measured at 1000 Hz in 0.1 M KCL containing 20 mM HEPES, pH 6.8.

Fig. 6 Bode plots for the PtO, PtO/OTS and PtO/OTS/Rh lectrodes measured at 0.4 V in 0.1 M KCl containing 20 mM HEPES pH 6.8.

Fig. 7 Model of a single surface-bound membrane formed by detergent dialysis on an alkylsilanated electrode surface.

Fig. 8 (a) Proposed equivalent circuit for surface-bound membrane electrode interface. (b) Simplified equivalent circuit valid at higher frequency region.

Fig. 9 Theoretical simulation of impedance spectra from the proposed equivalent circuit in figure 8a for curve fit to the spectra in figure 6.

Fig. 10 Capacitances of the n-Si/SiO_2, n-Si/SiO_2/OTS and n-Si/SiO_2/OTS/Rh electrodes measured at 1000 Hz in 0.1 M KCl containing 20 mM HEPES pH 6.8.

Fig. 11 Capacitances of the TiO_2, TiO_2/OTS and TiO_2/OTS/Rh electrodes measured at 1000 Hz in 0.1 M KCl containing HEPES pH 6.8.

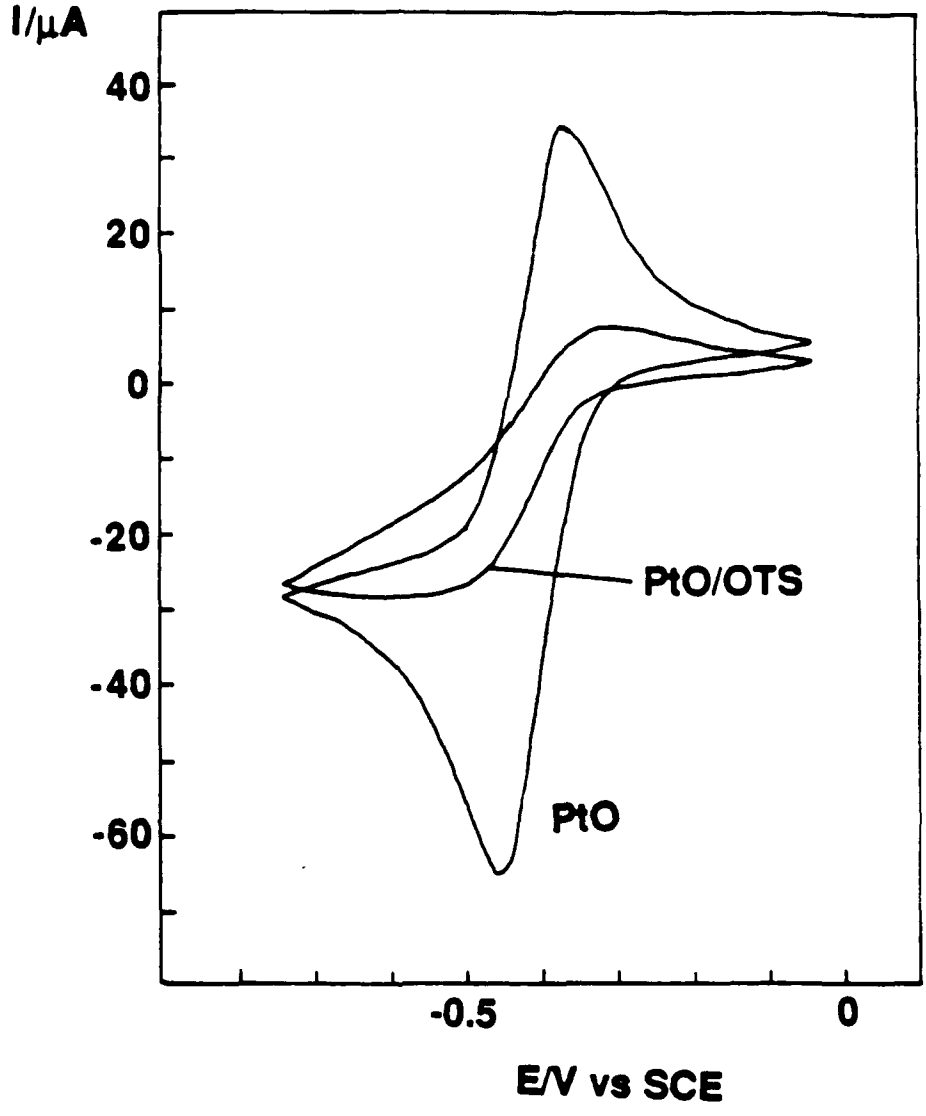
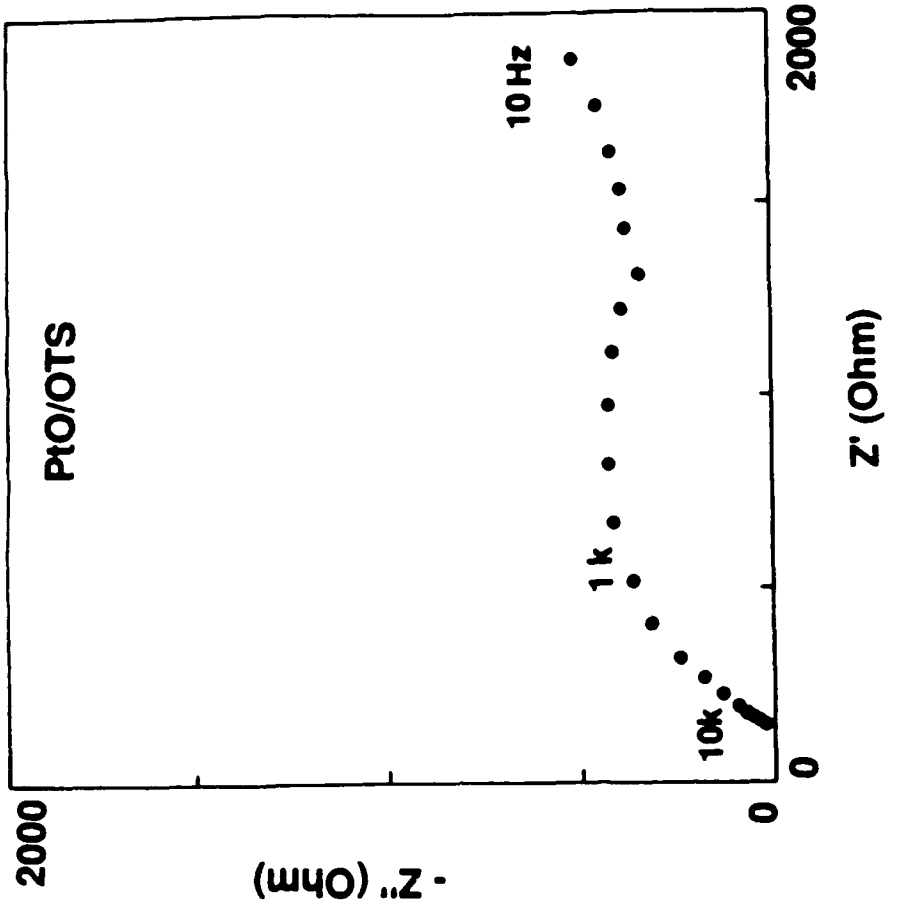


Figure 1


PtO/OTS
10 Hz
1 k
10k
2000
0
0
2000
- Z'' (Ohm)
Z' (Ohm)

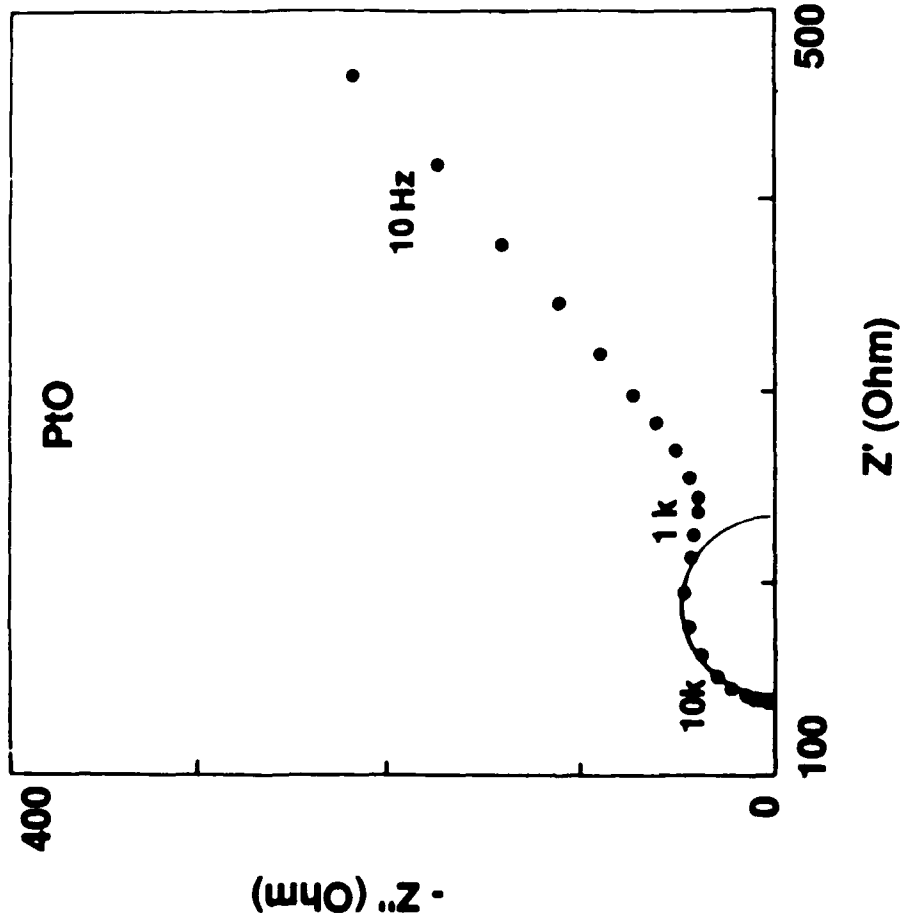

PtO
10 Hz
1 k
10k
500
100
0
400
- Z'' (Ohm)
Z' (Ohm)

Figure 2

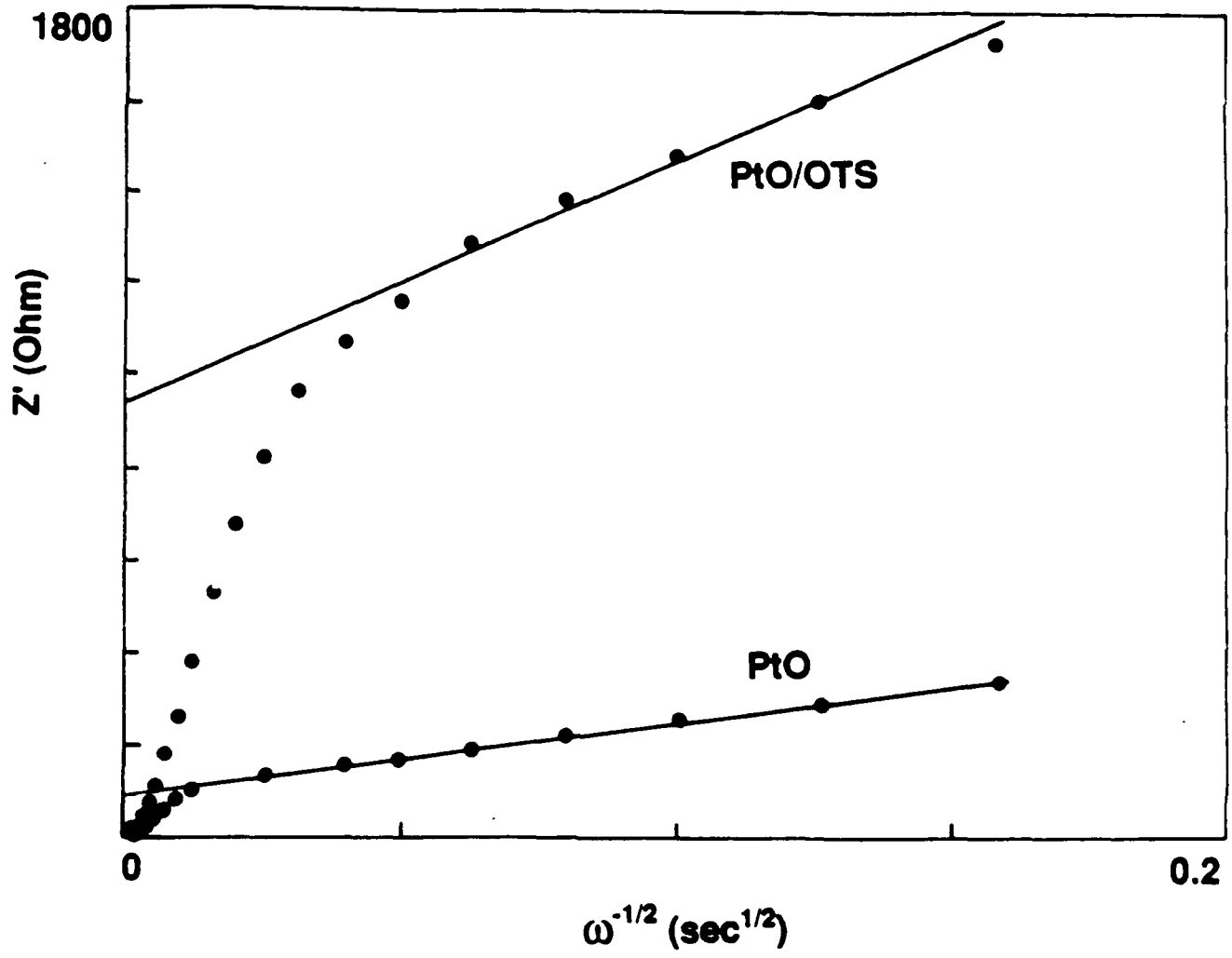


Figure 3

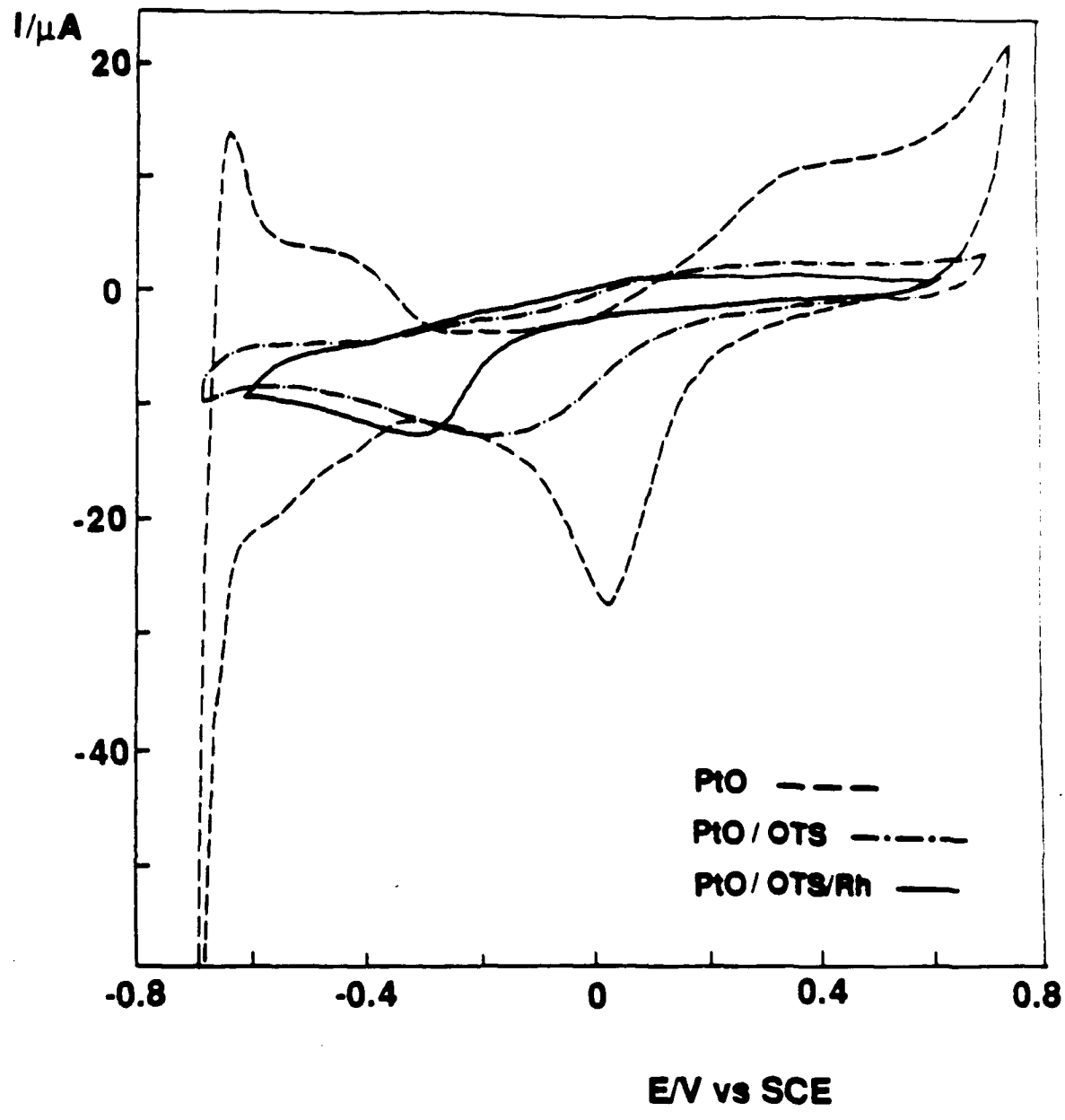


Figure 4

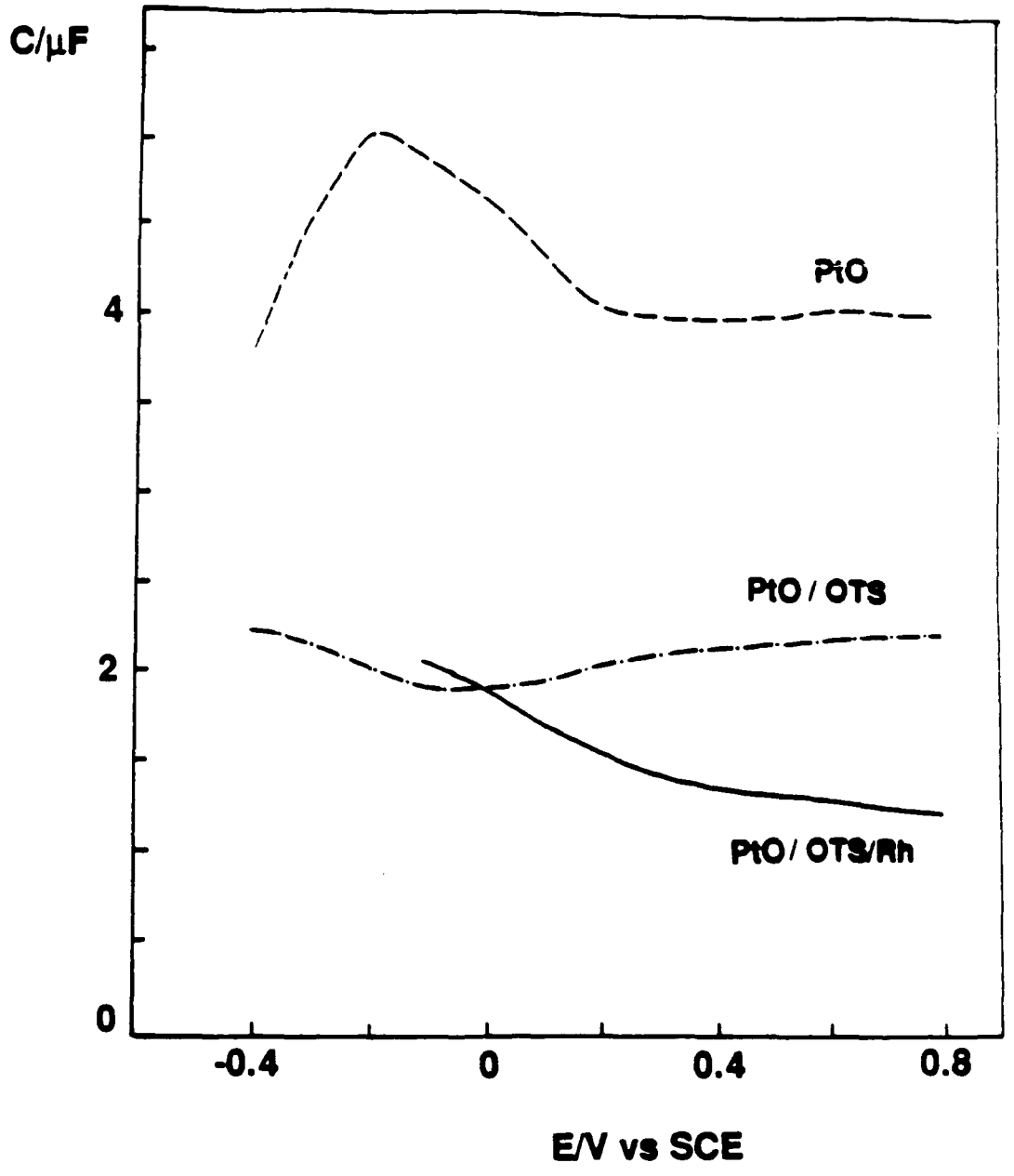


Figure 5

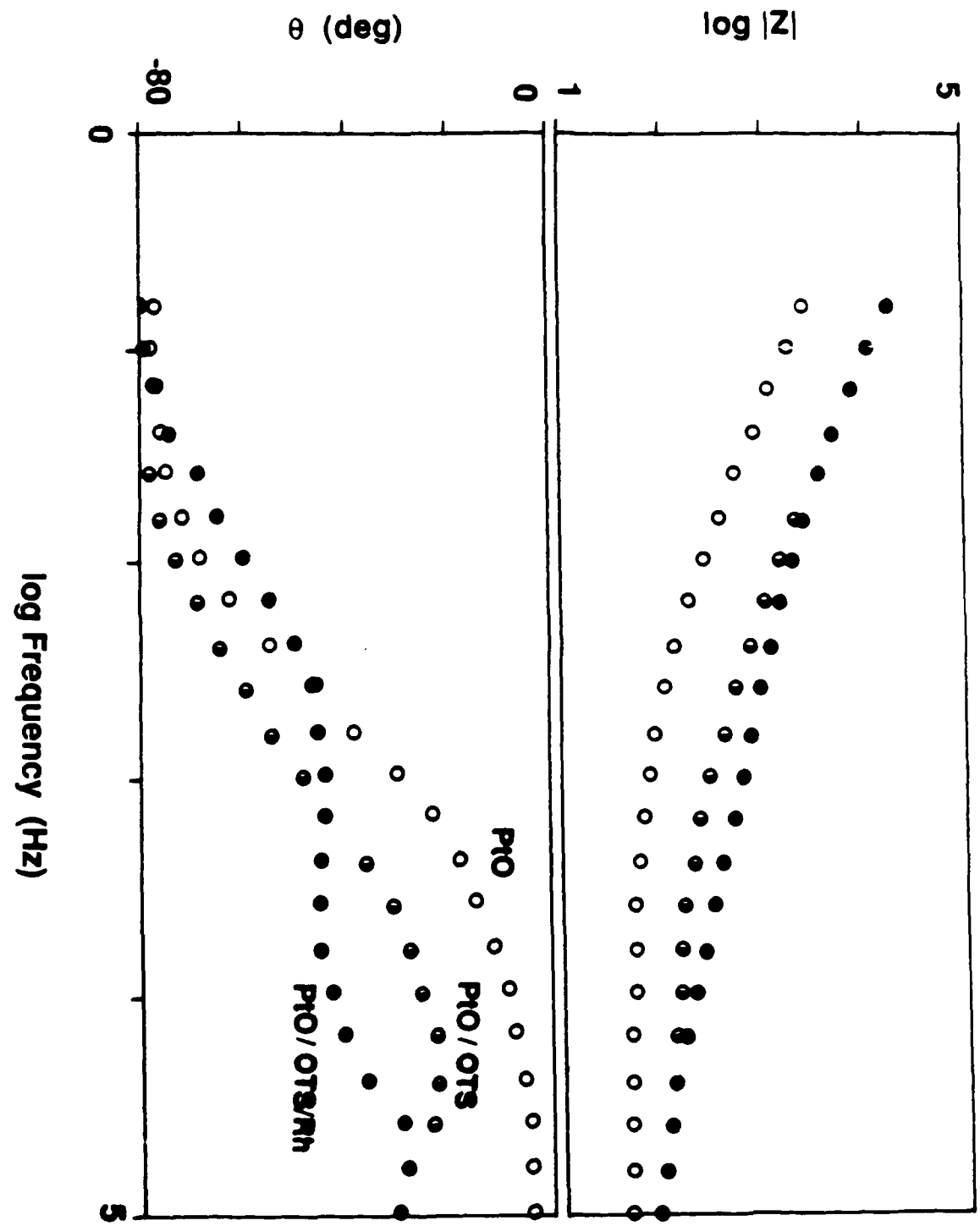


Figure 6

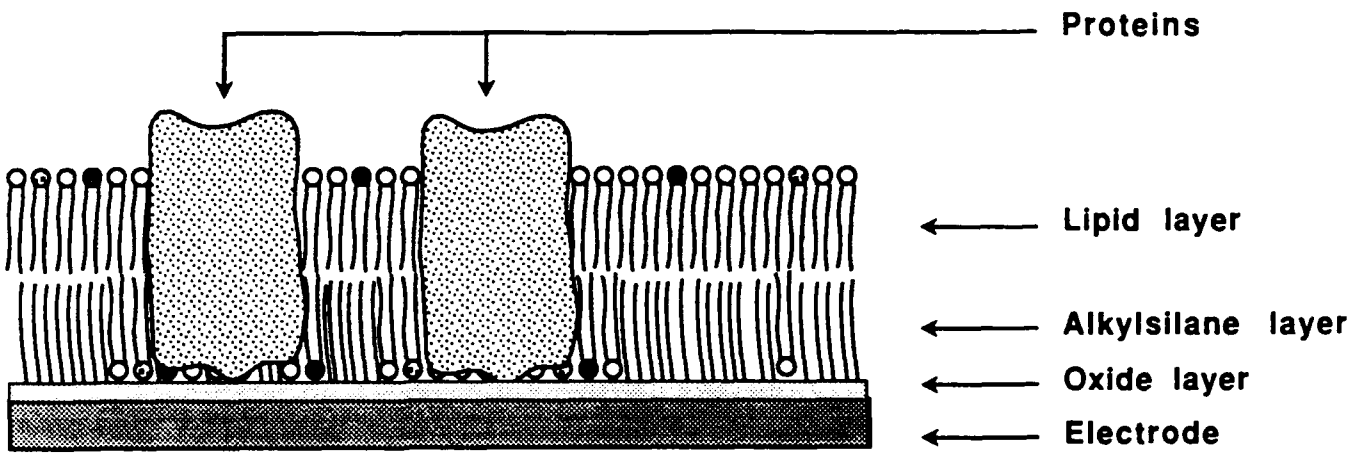

Proteins
Lipid layer
Alkylsilane layer
Oxide layer
Electrode

Figure 7

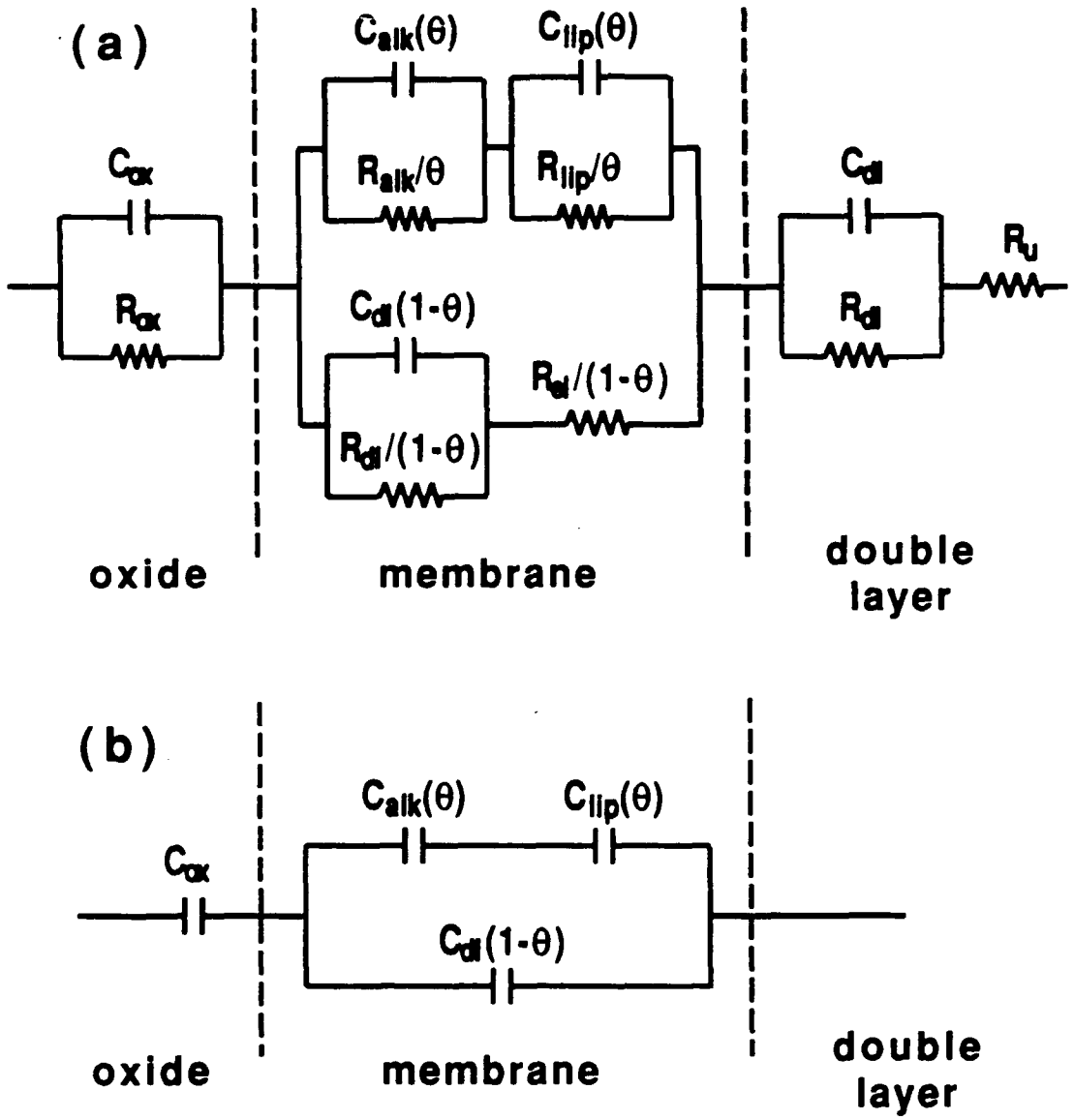

(a)
$C_{alk}(\theta)$
$C_{llp}(\theta)$
C_{ox}
R_{alk}/θ
R_{llp}/θ
C_{dl}
R_u
R_{ox}
$C_{dl}(1-\theta)$
R_{dl}
$R_{dl}/(1-\theta)$
$R_{dl}/(1-\theta)$
oxide
membrane
double layer
(b)
$C_{alk}(\theta)$
$C_{llp}(\theta)$
C_{ox}
$C_{dl}(1-\theta)$
oxide
membrane
double layer

Figure 8

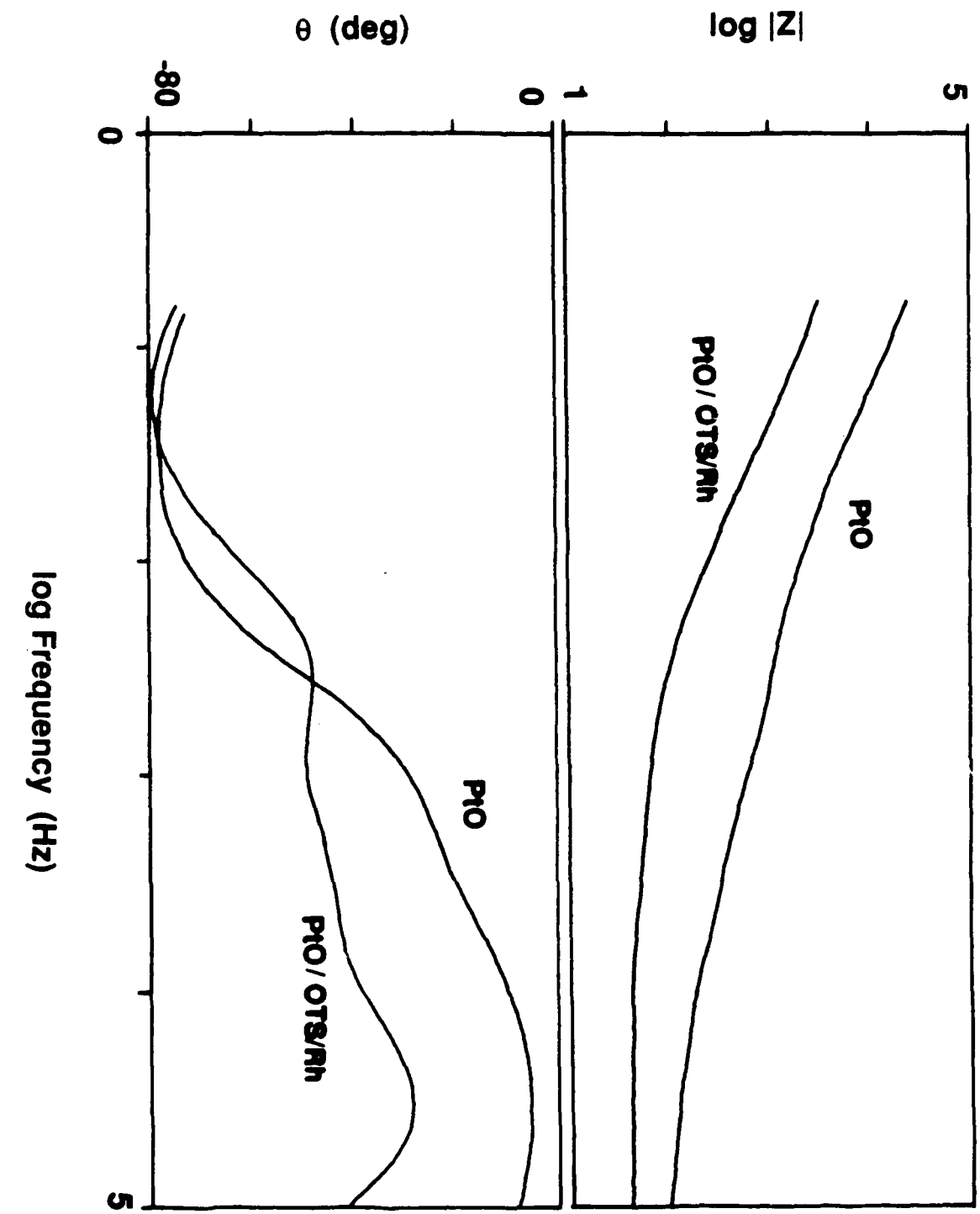

θ (deg)
-80
0
log |Z|
1
5
0
5
log Frequency (Hz)
PtO/OTS/Rh
PtO
PtO/OTS/Rh
PtO

Figure 3

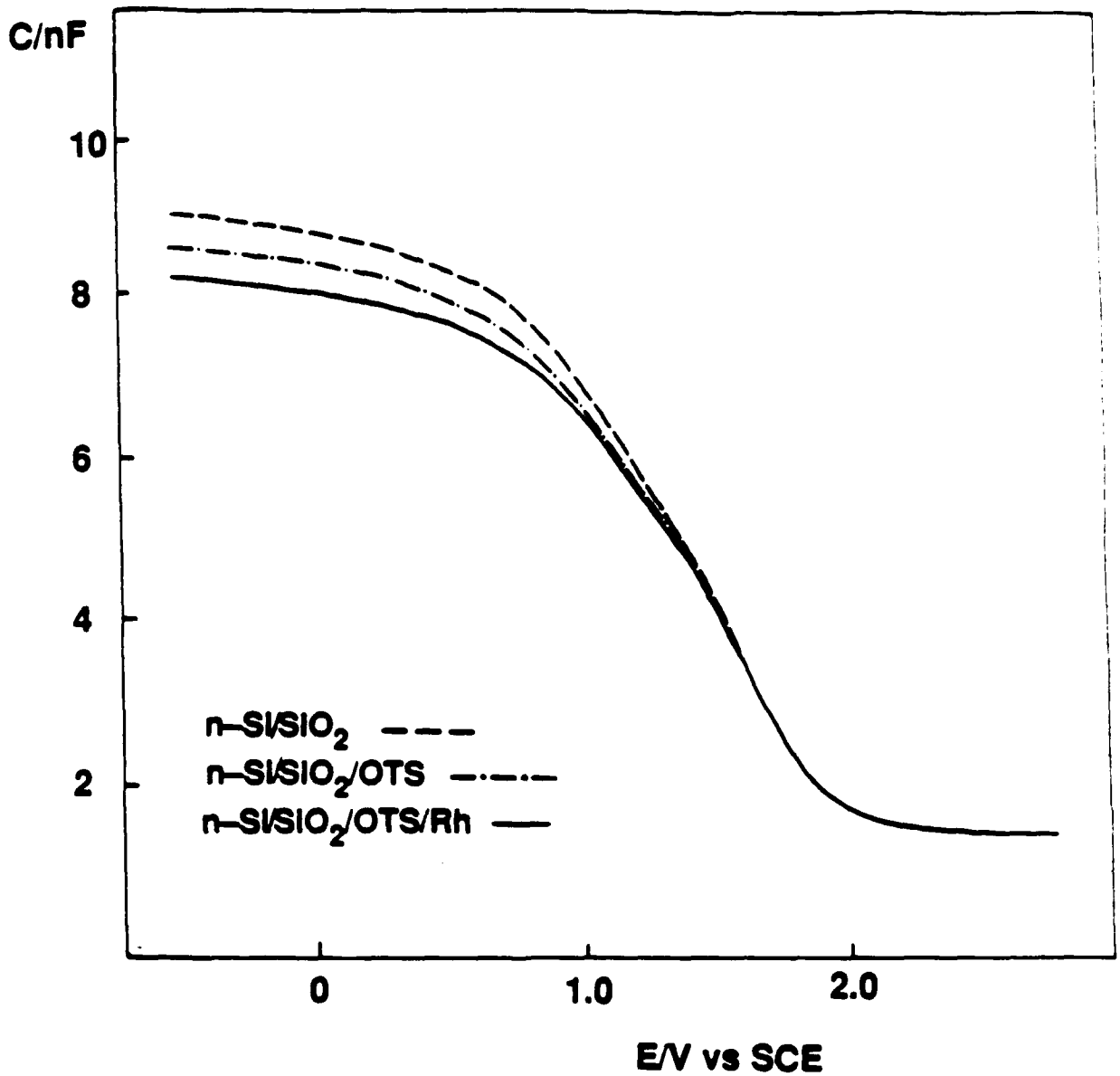

C/nF
10
8
6
4
2
n–Si/SiO2
n–Si/SiO2/OTS
n–Si/SiO2/OTS/Rh
0
1.0
2.0
E/V vs SCE

Figure 10

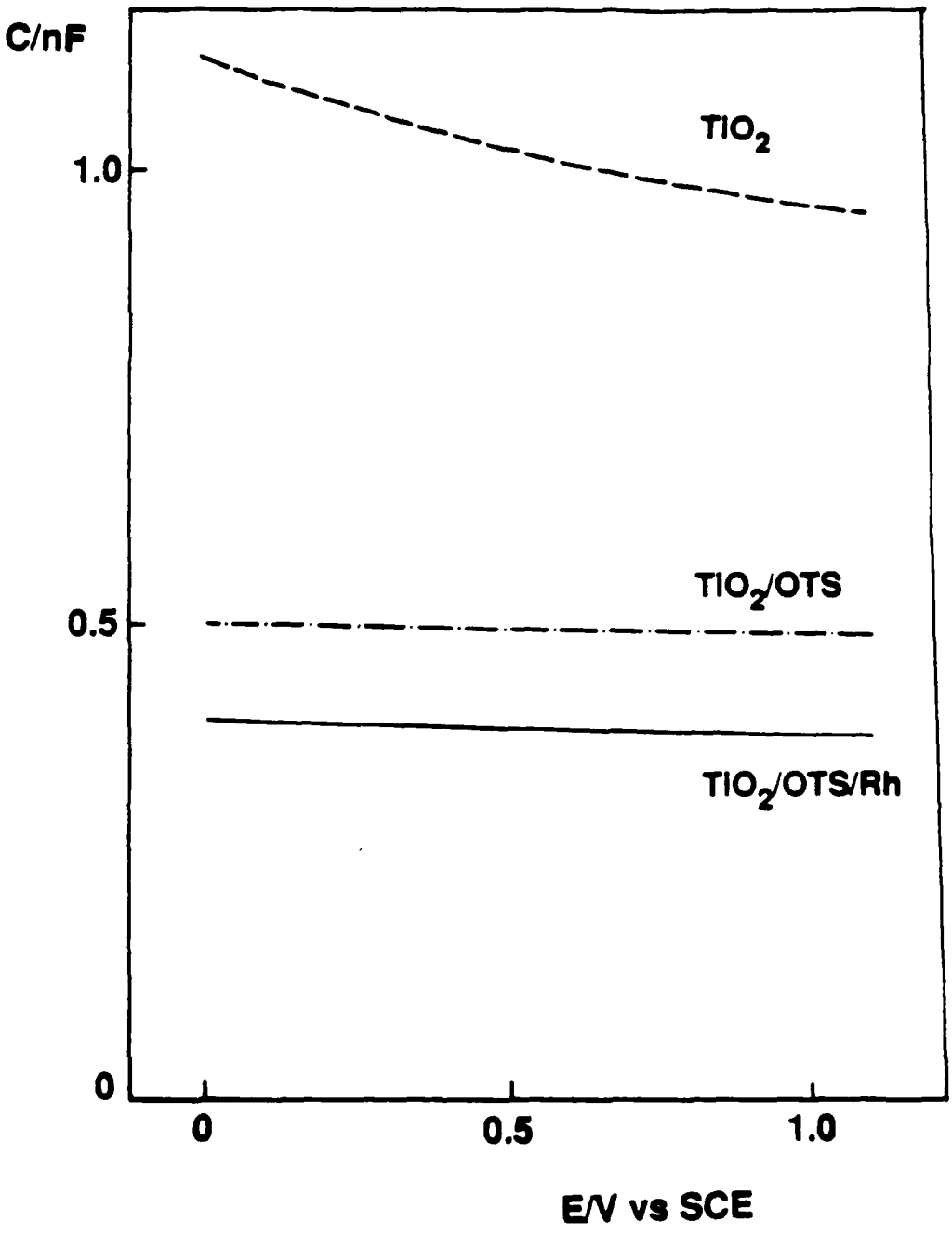


Figure 1'

Table 1. Parameters for best fit to impedance spectra (figure 6).

	Values for Model		Normalized Values	
PtO / membrane				
C_{dl}	2.5	μF	10	μF·cm^{-2}
C_{ox}	1.0	μF	4.0	μF·cm^{-2}
C_{alk}	0.25	μF	1.0	μF·cm^{-2}
C_{lip}	0.27	μF	1.1	μF·cm^{-2}
R_{ox}	800	Ω	200	Ω·cm^2
R_{alk}	3000	Ω	1200	Ω·cm^2
R_{lip}	500	Ω	125	Ω·cm^2
R_{dl}	80,000	Ω	20,000	Ω·cm^2
R_u	120	Ω	30	Ω·cm^2
R_{el}	12	Ω	3	Ω·cm^2
θ	0.97			
Bare PtO electrode				
C_{dl}	6.0	μF	24	μF·cm^{-2}
C_{ox}	3.0	nF	12	μF·cm^{-2}
R_{dl}	5000	Ω	1250	Ω·cm^2
R_{ox}	40	Ω	10	Ω·cm^2
R_u	80	Ω	20	Ω·cm^2

Table 2. Capacitances for Membranes formed on various Electrodes.

Type of Electrode	C-total (nF/cm²)*			C-layer (nF/cm²)**		C_{bl}† (nF/cm²)	Thickness‡ (Å)
	Bare	OTS	OTS/memb	OTS	OTS/memb		
PtO	10260	1100	800	1232	867	584	46.8
TiO_2	581	1120	607	3358	950	670	40.8
ITO	3020	1423	710	1490	926	645	42.4
p-Si/SiO_2	62.95	60.1	57	330	610	320	85.4
n-Si/SiO_2	40.7	39.7	39	1627	793	508	53.8

* Capacitance measured at 1000 Hz for unmodified electrode (Bare), after alkylsilanization (OTS), and after membrane deposition (OTS/memb).

** Calculated capacitance for each surface layer.

† Calculated capacitance of membrane using C_{dl} = 10 μF/cm² and θ = 0.97.

‡ Calculated using ε = 3.

TECHNICAL REPORT DISTRIBUTION LIST - GENERAL

Office of Naval Research (2)*
Chemistry Division, Code 1113
800 North Quincy Street
Arlington, Virginia 22217-5000

Dr. James S. Murday (1)
Chemistry Division, Code 6100
Naval Research Laboratory
Washington, D.C. 20375-5000

Dr. Robert Green, Director (1)
Chemistry Division, Code 385
Naval Weapons Center
China Lake, CA 93555-6001

Dr. Eugene C. Fischer (1)
Code 2840
David Taylor Research Center
Annapolis, MD 21402-5067

Dr. Elek Lindner (1)
Naval Ocean Systems Center
Code 52
San Diego, CA 92152-5000

Commanding Officer (1)
Naval Weapons Support Center
Dr. Bernard E. Douda
Crane, Indiana 47522-5050

Dr. Richard W. Drisko (1)
Naval Civil Engineering
Laboratory
Code L52
Port Hueneme, CA 93043

Dr. Harold H. Singerman (1)
David Taylor Research Center
Code 283
Annapolis, MD 21402-5067

Chief of Naval Research (1)
Special Assistant for Marine
Corps Matters
Code 00MC
800 North Quincy Street
Arlington, VA 22217-5000

Defense Technical Information
Center (2)
Building 5, Cameron Station
Alexandria, VA 22314

Office of Naval Research (1)
Biological Sciences Division
ATTN: Dr. Igor Vodyanoy, Code 1141SB
800 N. Quincy St.
Arlington, VA 22217-5000